Search for the Higgs Boson in Dilepton plus Missing Transverse Energy Final State with the DØ Detector at $\sqrt{s} = 1.96$ TeV

Ruchika Nayyar (for the DØ collaboration)
University of Delhi, India

We present a search for the standard model (SM) Higgs boson optimized in the decay channel $H \to W^+W^-$, where both W bosons decay leptonically. The final state considered contains dilepton and missing transverse energy from the neutrinos. A multivariate analysis is used to suppress the background. No significant excess above the SM background has been observed and limits on the Higgs boson production cross section times the branching ratio for $m_H = 115 - 200$ GeV are computed. Results using 8.1 fb^{-1}of data are presented.

1 Introduction

In this search channel, final states containing two leptons ($e^{\pm}\mu^{\mp}$, e^+e^- or $\mu^+\mu^-$) and missing transverse energy are considered. The production of Higgs boson by gluon fusion, vector boson fusion (VBF) and production in association with a vector boson (W/ZH) are considered. The preselection, based on the efficient reconstruction of the two leptons, is followed by additional requirements to suppress the large Drell Yan (DY) $Z/\gamma^* \to \ell\ell$ background. A final multivariate analysis based on a random forest of decision trees (DT) is used to separate the signal from the remaining background. The DT output is used to search for the Higgs signal. The analysis relies on efficient reconstruction of objects using all sub-detectors of the Run II DØ detector [1].

2 Data and Monte Carlo Samples

The data sample used in this analysis was collected between April 2002 and December 2010 by the DØ detector at the Fermilab Tevatron collider at $\sqrt{s} = 1.96$ TeV, and corresponds to an integrated luminosity of 8.1 fb^{-1} after imposing data quality requirements. Signal and SM background processes are simulated either with Pythia [2] or Alpgen [3] using the CTEQ6L1 [4] PDFs, followed by a Geant-based [5] detector simulation. The generated events are normalized to the highest-order cross-section calculation available. The transverse momentum of the Higgs boson generated in the gluon fusion process is weighted to reproduce the higher-order calculation by Hqt, at NNLL and NNLO accuracy [6].

The main backgrounds to the final state are diboson production, $Z/\gamma^* \to \ell\ell$ decays, W+jets/γ production, $t\bar{t}$ decays and multijet.

For the W+jets and Z+jets backgrounds we use the Alpgen [3] event generator. In the ee and $e\mu$ channels, the W+jets sample includes contributions from events where a jet or photon is misidentified as an electron. The size of each of these contributions is corrected to match the data in the W+jets enhanced control sample. For the WW production, the p_{T} of the diboson

system is modeled using the MC@NLO simulation [7] and the distribution of the opening angle of the two leptons is corrected to take into account the contribution from gluon fusion [8]. The background due to multijet production where jets are misidentified as leptons, is determined from data.

3 Preselection

All events are required to have two oppositely charged leptons originating from the same position (within 2 cm) along the beam-line. In the e^+e^- channel, the leading electron is required to have $p_{\mathrm{T}} > 15$ GeV and the second electron is required to have $p_{\mathrm{T}} > 10$ GeV. In the $e^{\pm}\mu^{\mp}$ channel, the muon must have $p_{\mathrm{T}} > 10$ GeV while the electron is required to have $p_{\mathrm{T}} > 15$ GeV. In the $\mu^+\mu^-$ channel the leading muon is required to have $p_{\mathrm{T}} > 15$ GeV and the second muon must have $p_{\mathrm{T}} > 10$ GeV. The e^+e^- and $\mu^+\mu^-$ channel also applied a cut on the $\mathrm{M}_{ll} > 15$ GeV. This stage of the analysis is referred to as "preselection". Figures 1 show some kinematic distributions at preselection.

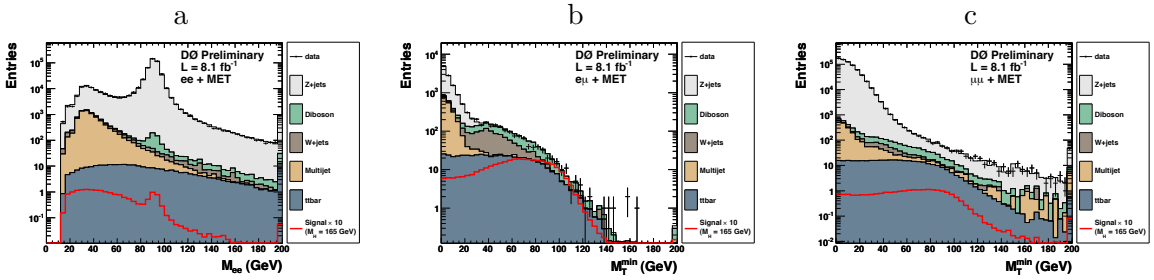

Figure 1: The (a) Dilepton mass, (b) $\not\!\!E_T$ and (c) minimum transverse mass between either lepton and the $\not\!\!E_T$.

To improve the sensitivity of the analysis, the preselection sample is further subdivided by the number of jets present in the event. Jets are required to have $p_{\mathrm{T}} > 20$ GeV, $|\eta| < 2.4$, pass quality requirements, and to have charged tracks associated with the primary $p\bar{p}$ vertex.

4 Final Selection

The Di-electron and Di-muon channel use a DT discriminant against the Z/γ^* background. The DT uses $\not\!\!E_T$ based variables to separate this dominant background. It is trained for each Higgs mass point considered in each jet bin. To reject most of this background, a cut is applied on this discriminant. The choice of the cut varies for each Higgs mass point in each jet bin. The electron-muon final state does not utilize such a discriminant and rather applies a cut on the minimum transverse mass, defined as:

$$M_T = \sqrt{2 \cdot \cdot \not\!\!E_T \cdot (1 - \cos\Delta\phi(\ell, \not\!\!E_T))}$$
$$M_T^{min} = min(\mathrm{M}_T^e, M_T^{\mu}) \quad (1)$$

The number of events at the final selection for the Dilepton states are shown in Table 1.

Table 1: Expected and observed number of events in each jet multiplicity after the final selection in all the final states. The signal assumes a Higgs boson mass of 165 GeV.

	Data	Total Background			Signal	$Z \to ee$	$Z \to \mu\mu$	$Z \to \tau\tau$	$t\bar{t}$	W+jets	Diboson	Multi-jet
$e\mu$:												
0 jets	1074	1163.5	±	145.4	16.0	16.9	74.7	89.9	14.1	462.8	473.2	31.9
1 jet	392	373.7	±	58.7	7.2	3.6	15.9	75.0	109.6	86.0	67.9	15.7
≥ 2 jets	280	285.7	±	41.4	3.2	1.1	3.9	21.8	220.6	24.2	10.2	3.9
ee:												
0 jets	676	715.8	±	89.9	7.2	108.5	-	9.1	6.1	376.8	205.3	10.0
1 jet	836	831.9	±	144.5	4.2	477.6	-	83.5	75.4	125.0	56.9	14.2
≥ 2 jets	477	442.6	±	73.9	2.4	201.7	-	42.9	160.8	13.9	17.1	6.2
$\mu\mu$:												
0 jets	612	689.7	±	60.7	9.3	-	201.8	2.7	3.8	136.6	240.6	104.2
1 jet	1420	1313.2	±	173.3	5.5	-	969.1	109.8	76.4	38.0	74.4	45.6
≥ 2 jets	888	890.8	±	135.4	3.7	-	579.6	46.8	209.4	7.2	28.2	19.5

5 Final Discriminant

After preselection, the signal is separated from the remaining background using an additional random forest decision tree (DT). Different discriminating variables such as b-tag information of the jets are employed to distinguish signal from background in various jet bins. The DT discriminant distributions for a Higgs boson mass of 165 GeV can be found in Fig.2.

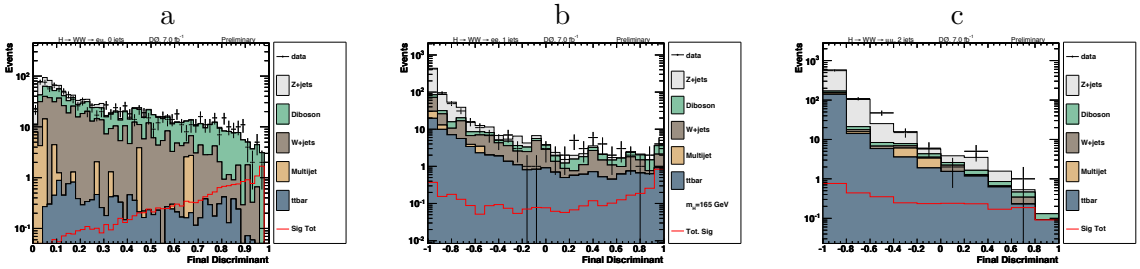

Figure 2: Final DT discriminant for (a)$e^+\mu^-$ in 0-jet bin, (b) e^+e^- in 1-jet bin and (c) $\mu^+\mu^-$ in $\geq$ 2-jet bin; The discriminant shown is trained for a Higgs mass of 165 GeV.

6 Systematic Uncertainties

The following sources of systematic uncertainty which affect only normalization are assessed: reconstruction efficiency for electrons (2.5% each) and muons (4% each); electron resolution (2% each); theoretical cross sections for Z+jets (6%), W+jets (6%), diboson (7%), and $t\bar{t}$(10%); multijet normalization (20%); W+jets overall normalization (20%); b-tagging in the heavy-flavor $t\bar{t}$ sample (5%) and remaining light-flavor samples (10%); and luminosity/normalization (6%). The signal $gg \to H$ cross-section has different cross-section and PDF uncertainties depending on the reconstructed jet bin: 0-jet (7% and 17.3%), 1-jet (23% and 29.7%) and 2-jet (33% and 30%). We also consider sources of systematic uncertainty which affect the shape of the final variable distribution (and quote here the average fractional change across bins of the final variable distribution for all backgrounds): jet energy scale (2.4%); jet resolution (3.8%); jet identification (2.1%); jet association to primary vertex (vertex confirmation) (1.7%).

Table 2: Expected and observed cross section $\sigma(p\overline{p} \to H + X)$ at 95 SM prediction for the Dilepton combination.

$M_H =$	115	120	125	130	135	140	145	150	155	160	165	170	175	180	185	190	195	200
Expected:	8.55	5.83	4.39	3.38	2.66	2.23	1.94	1.71	1.44	1.05	0.97	1.15	1.30	1.57	1.93	2.25	2.75	3.20
Observed:	9.95	9.12	8.06	4.97	4.25	3.45	3.83	2.85	2.73	1.61	0.91	1.55	1.65	1.91	2.56	2.93	3.55	4.15

7 Results and Conclusions

After the selection, the DT output distributions in data agree within the systematic uncertainties with the expected background prediction. Therefore the DT output distributions are used to set limits on the Higgs boson inclusive production cross section $\sigma(p\overline{p} \to H + X)$ assuming SM values for the branching ratios. Limits are calculated using a modified frequentist method (CLs), with a log-likelihood ratio (LLR) test statistic [9]. To minimize the degrading effects of systematics, the individual background contributions are fitted to the data observation by maximizing a profile likelihood function for each hypothesis [10].

Table 2 presents expected and observed upper limits at 95% CL. Figure 3a shows the expected and observed limits while Figure 3b shows the corresponding LLR distribution. At $M_H = 165$ GeV, the observed limit ratio is 0.91, with 0.97 expected, indicating that a standard model Higgs boson of this mass is excluded at the 95% CL.

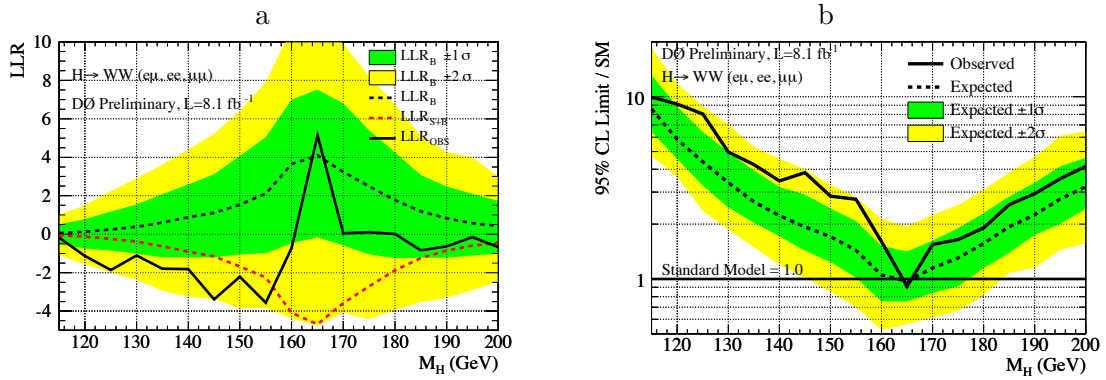

Figure 3: The observed LLR with the expected LLR for S and S+B hypothesis with green and yellow bands indicating one and two sigma bands is shown in (a) while (b) shows the excluded cross section ($\sigma(p\overline{p} \to H + X)$) at 95% CL in units of the SM cross section.

1. DØ Collaboration, V. Abazov *et al.*, Nucl. Instrum. Methods Phys. Res. A. **565**, 463 (2006).
2. T. Sjöstrand *et al.*, Comp. Phys. Comm. **135**, 238 (2001), we use version 6.323 or later.
3. M.L. Mangano, M. Moretti, F. Piccinini, R. Pittau, A. Polosa, JHEP **0307**, 001 (2003), we use version 2.11.
4. J. Pumplin et al., JHEP **07**, 012 (2002).
5. R. Brun and F. Carminati, CERN Program Library Long Writeup W5013, 1993 (unpublished).
6. G. Bozzi, S. Catani, D. de Florian, M. Grazzini, Phys. Lett.B 564 (2003) 65 [hep-ph/0302104]; Nucl. Phys. B 737 (2006) 73 [hep-ph/0508068].
7. S. Frixione and B.R. Webber, JHEP 0206 (2002) 029 [hep-ph/0204244].
8. T. Binoth, M. Ciccoli, N. Kauer, M. Krämer, JHEP **0503**, 065 (2005), JHEP **0612**, 046 (2006).
9. T. Junk, Nucl. Instrum. Methods Phys. Res. A. **434**, 435 (1999). A. Read, CERN 2000-005 (30 May 2000).
10. W. Fisher, FERMILAB-TM-2386-E.